NASA-CR-193079

Modulation and Coding for Throughput-Efficient Optical Free-Space Links

Costas N. Georghiades[1]
Electrical Engineering Department
Texas A&M University
College Station, Texas 77843-3128
Tel/Fax: (409)-845-7408/6259
e-mail: cng@cyprus.tamu.edu

Abstract

Optical direct-detection systems are currently being considered for some high-speed inter-satellite links, where data-rates of a few hundred megabits per second are envisioned under power and pulsewidth constraints. In this paper we investigate the capacity, cutoff-rate and error-probability performance of uncoded and trellis-coded systems for various modulation schemes and under various throughput and power constraints. Modulation schemes considered are on-off keying (OOK), pulse-position modulation (PPM), overlapping PPM (OPPM) and multi-pulse (combinatorial) PPM (MPPM).

[1]This work was supported by the NASA Lewis Research Center under grant NAG3-1353.

1 Introduction

Optical direct-detection systems have long been considered by NASA for deep-space communication, due to their small size and relatively high power efficiency [1]. For these low power, low data rate applications (a few tens of kilobits/s), good performance for little power is paramount; under these constraints, pulse-position modulation (PPM) was shown to be a well suited modulation scheme [2, 3]. PPM has also been the modulation of choice for NASA's direct-detection intersatellite link (ISL) applications for which quaternary PPM (QPPM) has been much studied [4, 5] for data rates of a few hundred megabits/s. In the future, even higher data rates are envisioned for which PPM may not be well suited due to its inherent throughput limitations: With PPM, the only way throughput can increase is by reducing the pulsewidth. Thus, if Q is the PPM alphabet size, T_s the slot duration (pulsewidth), and r the rate in nats per second, we have

$$rT_s = \frac{\ln(Q)}{Q} \leq \frac{\ln(3)}{3} \text{ nats/slot}, \tag{1}$$

which suggests ternary PPM can yield the largest throughput for a fixed pulsewidth T_s.

Thus, there is a motivation for investigating the use of other modulation schemes for high rate systems which, hopefully, do not have the limitations of PPM. One such scheme is overlapping PPM (OPPM) which was originally studied in [6] and later in [7, 8, 9]. OPPM is a generalization of PPM that allows more than one pulse-positions per pulsewidth and preserves some of the desirable properties of PPM, such as equal energy signals and low duty-cycle. If Q is the number of nonoverlapping pulse-positions in a T-second symbol interval (i.e. $Q = T/T_s$) and N (referred to also as the *index of overlap*) the number of pulse-positions per pulsewidth, then the total number of OPPM symbols J is $J = N(Q-1)+1$. For $N = 1$, OPPM reduces to PPM. If we constrain Q to be an integer, then to obtain a desirable number of modulation signals J, the index of overlap must be $N = (J-1)/(Q-1)$, which is a rational number. For r the rate in nats/s, the following is true for OPPM

$$rT_s = \frac{\ln[N(Q-1)+1]}{Q} \leq \frac{\ln(N+1)}{2} \text{ nats/slot}, \tag{2}$$

which (at least in theory) can be made as large as desired by increasing N. Clearly, there is a penalty to be paid when N is increased, both in error-probability and synchronization performance, which must be taken into account in comparing OPPM to other modulation schemes. Figure 1 illustrates OPPM for $N = 3$ and $Q = 2$, which results in $J = 4$ signals.

Another modulation scheme that has been considered recently in the literature is multipulse or combinatorial PPM (MPPM) [10, 11]. As with OPPM, MPPM is another generalization of PPM that allows more than one pulses per symbol interval. Thus, if the number of pulses allowed is p, the number of MPPM symbols is $M = \binom{Q}{p}$, which increases

monotonically for $1 \leq p \leq \lfloor Q/2 \rfloor$. Clearly, the interesting values of p are in the interval $1 \leq p \leq \lfloor Q/2 \rfloor$. Like PPM, MPPM is an equal energy signaling scheme, and like OPPM it increases the number of available signals for the same pulsewidth. For MPPM, the data rate relates to Q and p according to

$$rT_s = \frac{\ln\left[\binom{Q}{p}\right]}{Q} \quad \text{nats/slot.} \tag{3}$$

In view of some well known inequalities (see for example [12], page 284), we have,

$$h(p/Q) - \frac{\ln(1+Q)}{Q} \leq rT_s \leq h(p/Q) \quad \text{nats/slot,} \tag{4}$$

where $h(x) = -x\ln(x) - (1-x)\ln(1-x)$ is the binary entropy function. The ratio p/Q can be identified as the probability of a pulsed-slot in a sequence of MPPM symbols. As $Q \to \infty$, rT_s approaches $h(p/Q)$ which is the largest amount of information that can be produced by any binary source with prior symbol probabilities p/Q and $(1 - p/Q)$ [12]. Thus, at least asymptotically, MPPM is a throughput efficient scheme. For comparison, QPPM has a probability of a pulsed-slot of 1/4 and a throughput of $\ln(2)/2 = 0.346\cdots$ nats/slot. For the same probability of 1/4, MPPM can potentially achieve (for large Q) closed to $h(1/4) = 0.562\cdots$ nats/slot, a throughput increase of more than 60%.

In the next section, we derive capacity, cutoff-rate and error-probability expressions for OPPM and MPPM. Section 3 compares the various modulation schemes in terms of peak-power requirements and throughput efficiency. Section 4 gives a flavor of the coding problem over OPPM and MPPM symbols, and Section 5 concludes.

2 Error-Probability, Cutoff-Rate, and Capacity

Here we derive expressions for the error-probability, cutoff-rate, and capacity for MPPM and OPPM.

2.1 Multi-Pulse PPM

First we derive an expression for the optimum (maximum-likelihood) receiver for MPPM signals.

2.1.1 Optimum Receiver

Let $\mathcal{D} = \{d_k;\ k = 1, 2, \cdots, M\}$ be the set of all binary sequences of length Q having weight (number of ones) equal to p. Clearly, there is a one-to-one correspondence between binary sequences in $\mathcal{D}$ and MPPM signals, the position of ones in the binary sequence indicating the position of the pulsed slots in a (Q, p)-MPPM signal. Further, for the k-th MPPM signal

let $w_k = \{w_{k1}, w_{k2}, \cdots, w_{kp}\}$ be the set of integers from the set $\{1, 2, \cdots, Q\}$ indicating the position of the p ones, and $\overline{w}_k = \{\overline{w}_{k1}, \overline{w}_{k2}, \cdots, \overline{w}_{k(Q-p)}\}$ be the set integers indicating the position of the $(Q-p)$ zeros in that symbol. Finally, let $\mathbf{X} = (X_1, X_2, \cdots, X_Q)$ and $\mathbf{N} = (N_1, N_2, \cdots, N_Q)$ be the random vector of photons detected in each of the Q slots and a particular realization of it respectively. Clearly, the mean number of photons, Λ_i, in the i-th slot can take one of two values, depending on whether that slot is pulsed or not:

$$\Lambda_i = \begin{cases} (\lambda_s + \lambda_n)T_s & \text{if slot is pulsed} \\ \lambda_n T_s & \text{otherwise,} \end{cases} \tag{5}$$

where λ_s and λ_n are the signal and noise intensities respectively, and T_s is the slot duration.

A maximum-likelihood (ML) receiver then performs

$$\max_{d_k \in \mathcal{D}} \Pr(\mathbf{X} = \mathbf{N} | d_k). \tag{6}$$

Assuming Poisson statistics for the observed counts, we have

$$\begin{aligned} \Pr(\mathbf{X} = \mathbf{N} | d_k) &= \prod_{i=1}^{Q} \frac{e^{-\Lambda_i} \Lambda_i^{N_i}}{N_i!} \\ &= \frac{\exp(-\sum_{i=1}^{Q} \Lambda_i)}{\prod_{i=1}^{Q} N_i!} \prod_{i=1}^{p} [(\lambda_s + \lambda_n)T_s]^{N_{w_{ki}}} \prod_{j=1}^{(Q-p)} (\lambda_n T_s)^{N_{\overline{w}_{kj}}} \\ &= \exp(-\sum_{i=1}^{Q} \Lambda_i) \prod_{i=1}^{Q} \frac{(\lambda_n T_s)^{N_i}}{N_i!} \prod_{i=1}^{p} \left(1 + \frac{\lambda_s}{\lambda_n}\right)^{N_{w_{ki}}} \\ &= c \left(1 + \frac{\lambda_s}{\lambda_n}\right)^{\sum_{i=1}^{p} N_{w_{ki}}} \end{aligned} \tag{7}$$

where c is not a function of the data. Taking logarithms and dropping unnecessary terms, the receiver can equivalently implement

$$\max_{d_k \in \mathcal{D}} \ell_k \equiv \sum_{i=1}^{p} N_{w_{ki}}. \tag{8}$$

In other words, the receiver accumulates the number of photons in each pulsed slot for each possible transmitted symbol and declares the symbol corresponding to the one with the largest accumulated counts as the transmitted symbol.

Although the above analysis was done for PIN diode receivers, we can show that the same receiver is optimum for avalanche photodetectors.

2.1.2 Error-Probability

In this subsection we derive an exact expression for the symbol error-probability for a quantum-limited channel[2], and an upper bound on the symbol error-probability when background noise is present.

[2]An expression for the error-probability derived in [10] is not correct as it ignores the possibility of making a right decision even when one or more pulses are erased.

Quantum-Limited Channel: Assuming that all M symbols are equiprobable, we have

$$P(\mathcal{E}) = \frac{1}{M}\sum_{i=1}^{M} P(\mathcal{E}|d_i) = P(\mathcal{E}|d_1), \tag{9}$$

where the second equality is due to the symmetry of MPPM that implies $P(\mathcal{E}|d_i)$ is the same for all transmitted symbols d_i. Since for the quantum-limited channel errors occur only when one or more pulses are erased, we can write

$$P(\mathcal{E}) = \sum_{k=1}^{p} P(\mathcal{E}|\text{k erasures})P(\text{k erasures}). \tag{10}$$

When k pulses are erased, a random decision must be made among the $N_k \equiv \binom{Q-p+k}{k}$ symbols that have pulses at the $(p-k)$ positions were pulses were detected. Since the probability of exactly k erased pulses is $\binom{p}{k}\epsilon^k(1-\epsilon)^{p-k}$, we have

$$P(\mathcal{E}) = \sum_{k=1}^{p} \frac{N_k - 1}{N_k}\binom{p}{k}\epsilon^k(1-\epsilon)^{p-k}, \tag{11}$$

where

$$\epsilon = e^{-\lambda_s T_s} \tag{12}$$

is the pulse-erasure probability. An excellent approximation to (11) for ϵ less than approximately 10^{-2} is given by

$$P(\mathcal{E}) \approx \left(\frac{Q-p}{Q-p+1}\right)p\epsilon. \tag{13}$$

Background Noise Channel: For the noisy channel, we have

$$\begin{aligned} P(\mathcal{E}) &\leq P\left[\bigcup_{j=2}^{M}\{\ell_1 \leq \ell_j\}|d_1\right] \\ &\leq \sum_{j=2}^{M} P(\ell_1 \leq \ell_j|d_1), \end{aligned} \tag{14}$$

where the first inequality is obtained by assuming pessimistically that whenever equal counts occur an error is made, and the second follows from the union bound. Focusing on the probability inside the sum, we can show using the Chernoff bound that

$$P(\ell_1 \leq \ell_j|d_1) \leq \exp\left[-\frac{1}{2}d^2 d_H(d_1, d_j)\right], \tag{15}$$

where

$$d^2 = \left(\sqrt{(\lambda_s+\lambda_n)T_s} - \sqrt{\lambda_n T_s}\right)^2, \tag{16}$$

and $d_H(d_1, d_j)$ is the Hamming distance between d_1 and d_j.

To proceed further, we need to find the Hamming distance profile for the MPPM signals. Towards this end, we first note that the possible values that $d_H(d_1, d_j)$ can take are $2, 4, \cdots, 2p$. Further study using counting arguments shows that if a_k, $k = 1, 2, \cdots, p$ is the number of symbols at distance $2k$ from d_1, then

$$a_k = \binom{p}{k}\binom{Q-p}{k}. \tag{17}$$

In fact, it can be shown that because of the symmetry of the MPPM signals noted above, we have the same distance profile when any signal d_i is sent (not just when d_1 is sent). It can be easily verified that $\sum_{k=1}^{p} a_k = M - 1$. Thus, the $(M-1)$ terms in the sum in (14) can be partitioned into groups of a_k terms each, for each of which the Chernoff-bound in (15) equals $\exp(-kd^2)$. Under these observations, equations (14) and (15) combine to give

$$P_{\text{mppm}}(\mathcal{E}) \leq \sum_{k=1}^{p} a_k e^{-kd^2}. \tag{18}$$

The general observation to be made from the above derivation is that what determines the performance of MPPM signals (at least for large signal levels when the bound above is tight) is the minimum Hamming distance between symbols. We will use this observation in Section 4 in determining the performance of trellis-coded MPPM signals.

2.1.3 Cutoff-Rate

We make use of the following general expression for the cutoff- rate derived in [3], valid for optical channels with observations modeled by conditional Poisson processes and both for quantum-limited[3] and noisy channels

$$R_0 = -\ln\left\{\min_{\{q_i\}} \sum_{i=1}^{M}\sum_{j=1}^{M} q_i q_j \exp(-\frac{1}{2}d_{ij}^2)\right\} \quad \text{(nats/cu)}, \tag{19}$$

where M is the number of MPPM signals, q_i is the prior probability for the i-th signal and

$$d_{ij}^2 = \int_0^T \left[\sqrt{s_i(t)+\lambda_n} - \sqrt{s_j(t)+\lambda_n}\right]^2 dt. \tag{20}$$

In (20), $[s_i(t)+\lambda_n]$ in photons/sec is the mean rate (intensity) of the observed Poisson process when the i-th signal is sent, $s_i(t)$ is the *signal intensity* due to the optical beam impinging on the photodetector, and λ_n is the *noise intensity* as defined previously.

For MPPM signals, we can express (20) as

$$d_{ij}^2 = d^2 d_H(d_i, d_j) \tag{21}$$

[3]Although expressions for the cutoff-rate and capacity for MPPM were derived in [13] for quantum-limited channels ($\lambda_n = 0$), we found that these expressions significantly underestimate the cutoff-rate and capacity of the channel, because of the pessimistic way erasures were defined.

where d^2 and $d_H(d_i, d_j)$ were defined above.

Then, for equiprobable signaling, the cutoff-rate becomes

$$\begin{aligned} R_0 &= -\ln\left[\frac{1}{M^2}\sum_{i=1}^{M}\sum_{j=1}^{M} e^{-\frac{1}{2}d^2 d_H(d_i,d_j)}\right] \\ &= -\ln\left[\frac{1}{M}\sum_{i=1}^{M} X_i\right], \end{aligned} \tag{22}$$

where

$$X_i = \frac{1}{M}\sum_{j=1}^{M} e^{-\frac{1}{2}d^2 d_H(d_i,d_j)}. \tag{23}$$

Using the symmetry of the MPPM signal set, we can show that $X_i = X_k$ for all i and k. Further, using the results in the previous subsection, we can write

$$X_i = \frac{1}{M}\sum_{k=0}^{p} a_k e^{-kd^2}, \tag{24}$$

and thus

$$R_{0\text{mppm}} = -\ln\left[\frac{1}{M}\sum_{k=0}^{p} a_k e^{-kd^2}\right], \tag{25}$$

with a_k defined above.

It is easy to verify that for $p = 1$, the above expression yields the cutoff-rate of Q-ary PPM.

2.1.4 Capacity

The MPPM direct-detection channel can be modeled as a discrete memoryless channel (DMC) with $M = \binom{Q}{p}$ inputs and L outputs. For a quantum-limited channel where the only degradation occurs when $1, 2, \cdots, p$ pulses are erased, the number of outputs equals the number of binary codewords of length Q and weight at most p. Thus,

$$L = \sum_{k=0}^{p}\binom{Q}{k}.$$

Of the L possible outputs, $\binom{Q}{p}$ correspond to the input symbols and the rest to words containing one or more erasures. An example of a DMC model for MPPM with $Q = 4$ and $p = 2$ is shown in Figure 3. The capacity of the channel is given by

$$C_{\text{mppm}} = \max_{P(x)}\sum_{i=1}^{M}\sum_{j=1}^{L} P(y_j|x_i)P(x_i)\ln\left(\frac{P(y_j|x_i)}{P(y_j)}\right). \tag{26}$$

Due to the easily established symmetry of the channel, (see Cover [12], Section 8.2, or Gallager [15]), the maximizing prior distribution is uniform, $P(x_i) = 1/M$, $i = 1, 2, \cdots, M$.

Further, it can be seen that the inside sum in (26) is the same for each x_i. Skipping the derivations, we finally obtain

$$C_{\text{mppm}} = \sum_{k=0}^{p} \binom{p}{k} \epsilon^k (1-\epsilon)^{p-k} \ln\left(\frac{M}{\binom{Q-p+k}{k}}\right) \tag{27}$$

$$= \ln(M) - \sum_{k=0}^{p} \binom{p}{k} \epsilon^k (1-\epsilon)^{p-k} \ln\left(\binom{Q-p+k}{k}\right). \tag{28}$$

The expression is easily seen to simplify to that of PPM for $p = 1$.

2.2 Overlapping PPM

In this subsection we present expressions for the error-probability, cutoff-rate, and capacity of OPPM. The optimum receiver for OPPM was derived in [8] and (as expected) consists of finding the slot with the largest number of observed photons.

2.2.1 Error-Probability

Quantum-Limited Channel: An exact expression[4] for the error probability has been derived in this case for N in the range from one to four and arbitrary J. In all of these cases it can be shown (we skip the derivations here as they are somewhat tedious but otherwise straightforward) that

$$P(\mathcal{E}) = \frac{J-1}{J} \exp(-\frac{\lambda_s T_s}{N}), \tag{29}$$

where $J = N(Q-1)+1$ is the OPPM alphabet size. Computation for larger values of N is easy but becomes progressively more tedious. Based on the results for the values of N considered, we conjecture that the above expression is true for all N.

Background Noise Channel: When background noise is present, the following upper-bound was derived in [8] which we present here for completeness

$$P_{\text{oppm}}(\mathcal{E}) \leq \frac{1}{J} \sum_{k=1}^{N} b_k e^{-kd^2/N} \tag{30}$$

where

$$b_k = \begin{cases} 2(J-k), & k = 1, 2, \cdots, (N-1) \\ (J-N)(J-N+1) & k = N, \end{cases} \tag{31}$$

and d^2 is as defined in (16).

[4] An expression derived in [8] for the error probability is exact only for $N = 2$, and an approximation otherwise.

2.2.2 Cutoff-Rate

Here again we make use of (19). Using (20) we can write

$$d_{ij}^2 = \frac{2d^2}{N}\delta_{ij} \tag{32}$$

where d^2 is as defined in (16) and

$$\delta_{ij} = \begin{cases} |i-j|, & \text{if } |i-j| \le N \\ N, & \text{if } |i-j| > N. \end{cases} \tag{33}$$

Note that for $i \neq j$ δ_{ij} takes values in $\{1, 2, \cdots, N\}$; if we consider the number of pairs i, j for which $\delta_{ij} = k$, then we can show that it is equal to b_k given in (31). Letting

$$\gamma = e^{-d^2/N} \tag{34}$$

and assuming equiprobable symbols we obtain (for $Q > 1$)

$$\begin{aligned} R_0 &= -\ln\left\{\frac{1}{J} + \frac{1}{J^2}\sum_{k=1}^{N} b_k \gamma^k\right\} \\ &= -\ln\left\{\frac{1}{J} + \frac{(J-N)(J-N+1)}{J^2}\gamma^N + \frac{2}{J}\frac{\gamma(1-\gamma^{N-1})}{1-\gamma} + \frac{2}{J^2}\left[\frac{N\gamma^N}{1-\gamma} - \frac{\gamma(1-\gamma^N)}{(1-\gamma)^2}\right]\right\}. \end{aligned} \tag{35}$$

For the noiseless case, i.e. $\lambda_n = 0$, (35) holds by substituting $d^2 = \lambda_s T_s$, which implies that $\gamma = e^{-\lambda_s T_s/N}$ is the *erasure* probability for signaled chips of duration T_s/N. Even though more general than the expression obtained in [7] (valid only when $\lambda_n = 0$), (35) is much simpler to compute.

In the limit as $N \to \infty$, (35) reduces to

$$\begin{aligned} R_{0\infty} &= -\ln\left\{\left(\frac{Q-2}{Q-1}\right)^2 \epsilon' + \frac{2(1-\epsilon)}{(Q-1)d^2} + \frac{2\epsilon'}{(Q-1)^2 d^2} - \frac{2(1-\epsilon')}{(Q-1)^2 d^4}\right\} \\ &\approx \ln\left[\frac{(Q-1)d^2}{2}\right], \quad Q > 1, \end{aligned} \tag{36}$$

where $\epsilon' = e^{-d^2}$. The approximation in (36) is valid for large values of d^2 and was also derived in [7] for quantum-limited channels.

2.2.3 Capacity

The capacity of OPPM was derived in [7] for a quantum-limited channel and is given here for reference

$$C_{\text{oppm}} = \sum_{i=2}^{N}\sum_{j=i-1}^{N-1}\sum_{k=1}^{J+N-j-1} c(k,j)\ln[c(k,j)]\gamma^{N-i}(1-\gamma)^i \binom{j-1}{i-2}$$

$$+ \gamma^{N-1}(1-\gamma) \sum_{k=1}^{J+N-1} c(k,0) \ln[c(k,0)] \tag{37}$$

where

$$c(k,j) = \frac{1}{J} \min(k, N-j, J+N-k-j). \tag{38}$$

2.3 On-Off Keying

Finally, for comparison purposes we present the cutoff-rate and error-probability of OOK, which was not in the past considered for free-space applications. The main reason for not considering OOK in such applications is the possibility of getting long sequences of ones or zeros that degrade synchronization performance, and in the former case require the laser to be on for a long time. Both problems are solvable, if one is willing to sacrifice some throughput through the use of appropriate line coding, but we will not pursue this in this paper.

The well known expression for the cutoff-rate for OOK, achieved with equiprobable signaling, is

$$R_{0\text{ook}} = \ln\left[\frac{2}{1+e^{-\lambda_s T_s/2}}\right], \tag{39}$$

and the error-probability is

$$P_{\text{ook}}(\mathcal{E}) = \frac{1}{2} e^{-\lambda_s T_s}. \tag{40}$$

The capacity of OOK is attained by a non-uniform prior distribution and is given by

$$C_{\text{ook}} = \ln\left[(1-\epsilon)\epsilon^{\frac{\epsilon}{1-\epsilon}} + 1\right]. \tag{41}$$

3 Performance Comparisons

In this section we use the expressions derived above to compare the performances of the various modulation schemes in terms of power-efficiency for a given throughput, capacity and cutoff-rate and peak power requirements. We address coded error-probability performance in the section that follows.

3.1 Power Efficiency

For coded systems, the capacity is a *fundamental* limit on the rates for reliable communication: below capacity error-probability can be made as small as desired by the use of (possibly very complex) coding, whereas above capacity this is not possible, no matter how complex the code [12, 15]. Although rates up to capacity are *theoretically* possible, researchers have found that coding complexity increases significantly at rates approaching capacity. In contrast, it was argued by Wozencraft and Kennedy [16] and Massey [17] that the cutoff-rate

of a system, which is upper-bounded by capacity, yields a *practical* limit on code rates for reliable communication. In this subsection we will use both the cutoff-rate and capacity as indicators of the achievable rates in order to investigate the throughput efficiencies of OOK, PPM, OPPM and MPPM.

Following [18, 19], we let r be the desired throughput in nats per second and T_s the desired pulsewidth. Both constraints stem from practical considerations where a certain throughput is required but the pulsewidth cannot be reduced beyond some limit. Fixing the throughput and the pulsewidth implies the following constraining equation (since $T = QT_s$ for PPM, MPPM and OPPM)

$$rT_s = \frac{R_0}{Q} \quad \text{nats/slot.} \tag{42}$$

For a fixed average noise photons per symbol, $\mathcal{L}_n$, and a fixed overlap N for OPPM or a fixed p for MPPM, (42) can be satisfied by varying the average number of signal photons/symbol $\mathcal{L}_s$, where for PPM and OPPM, $\mathcal{L}_s = \lambda_s T_s$ and for MPPM, $\mathcal{L}_s = p\lambda_s T_s$. If we let $\mathcal{L}_s(Q, rT_s, h)$ (where $h \equiv N$ for OPPM and $h \equiv p$ for MPPM) be the value of $\mathcal{L}_s$ satisfying (42), then the throughput efficiency in nats per photon is

$$R_{0ph} = \frac{R_0}{\mathcal{L}_s(Q, rT_s, h)} = \frac{rT_s Q}{\mathcal{L}_s(Q, rT_s, h)} \quad \text{nats/photon.} \tag{43}$$

In the following, we assume a quantum-limited channel for simplicity and also because at the high data rates envisioned for ISL systems only a small fraction of a noise photon is expected per slot (assuming the sun is not in the field of view) [14].

In general, explicit analytical solution of (42) for $\mathcal{L}(Q, rT_s, h)$ is not possible, except for some special cases, such as for PPM, $p = 2$ MPPM and $N = 2$ OPPM, for which:

$$R_{0ph} = \frac{rT_s Q}{\ln(Q-1) - \ln\left[Q\exp(-rT_s Q) - 1\right]}, \quad \text{PPM} \tag{44}$$

$$R_{0ph} = \frac{rT_s Q}{2\ln(Q-3) - 2\ln\left[\sqrt{\frac{(Q-1)}{(Q-2)}}\left[Q(Q-3)\exp(-rT_s Q) + 2\right] - 2\right]}, \quad \text{MPPM}, p = 2, \tag{45}$$

$$R_{0ph} = \frac{rT_s Q}{2\ln(2Q-3) - 2\ln\left[\sqrt{\frac{(2Q-1)^2(2Q-3)}{2(Q-1)}}\exp(-rT_s Q) - \frac{(4Q^2-10Q+5)}{2(Q-1)}} - 1\right] \quad \text{OPPM}, \ N = 2. \tag{46}$$

For OOK,

$$R_{0ph} = \frac{2rT_s}{\lambda_s T_s} = \frac{rT_s}{-\ln\left[2e^{-rT_s} - 1\right]} \leq 1/2. \tag{47}$$

The denominator of the above equations corresponds to the value of $\mathcal{L}_s(Q, rT_s, h)$ that satisfies (42). For values of p and N other than two, numerical solutions are easily obtained.

Figures 4 and 5 plot R_{0ph} in (43) for OPPM and MPPM respectively. For each modulation scheme and a given rT_s and N or p, there is an optimum value of Q that maximizes the throughput efficiency in nats/photon. Both OPPM ($N > 1$) and MPPM ($p > 1$) outperform PPM ($N = 1$ or $p = 1$). The improvement however of MPPM over PPM is only marginal and it comes at the price of having to use larger values of Q with increasing p to achieve the optimum efficiency. The latter is a drawback as large values of Q result in large signal sets which in turn make implementation more difficult. OPPM performs significantly better than PPM even with a small overlap $N = 2$ and requires relatively small values of Q to reach optimum efficiency.

A comparison between PPM, OPPM, MPPM and OOK as a function of the required nats/slot is made in Figure 6. The values of Q in the plot are optimum for the corresponding rT_s. Both MPPM and OPPM outperform PPM, especially at high throughputs. $N = 2$ OPPM is uniformly better than $p = 2$ MPPM but becomes worse than $p = 4$ MPPM as the throughput increases. For OPPM, we plot the two extreme overlap cases: $N = 2$ and $N = \infty$. Most of the gain in allowing overlap is obtained for $N = 2$, with progressively less incremental improvement as N is increased. OOK does poorly for small required *nats/slot*, but becomes better at high rates, outperforming all other schemes above rates of 1/2 nats/slot. For a practical comparison, let us consider the efficiencies of each modulation scheme at the rate of $\ln(2)/2 \approx 0.35$ nats/slot, which is the rate at which the currently developed QPPM system is at. At this rate, PPM has an efficiency of 0.284, OOK 0.392, $N = 2$ OPPM 0.528, $p = 2$ MPPM 0.482, and $p = 4$ MPPM 0.533. Clearly, all modulation schemes can do better than QPPM, whose performance is upper-bounded by 0.284 nats/photon (since this is the value obtained by the optimum value of $Q = 3$ for PPM).

Results similar to the above using the capacity instead of the cutoff-rate are shown in Table 1. For PPM, $N = 2$ OPPM, and $p = 2$ MPPM these results were obtained by using equations, which parallel those in equations (44)-(46). We present below the equations for PPM and $p = 2$ MPPM and skip the one for $N = 2$ OPPM as it is rather long. For OOK, no closed form expression is available.

$$C_{ph} = \frac{-rT_sQ}{\ln\left[\frac{\ln(Q)-rT_sQ}{\ln(Q)}\right]}, \quad \text{PPM} \tag{48}$$

$$C_{ph} = \frac{-rT_sQ}{2\ln\left[\frac{\ln(Q-1)-\sqrt{rT_sQ\ln[2(Q-1)/Q]+\ln^2(2/Q)}}{\ln[2(Q-1)/Q]}\right]}, \quad \text{MPPM}, p = 2. \tag{49}$$

In general, the capacity results are qualitatively similar to those using the cutoff-rate, with some exceptions. For example, whereas $N = 2$ OPPM is uniformly superior to $p = 2$ MPPM in Figure 6, Table 1 indicates that the latter is slightly better than the former for the smaller values of rT_s. The optimizing values of Q, also shown in the table, are closely similar to those obtained using the cutoff-rate. Finally, OOK which performs poorly for low

throughputs, outperforms significantly $N = 2$ OPPM and $p = 2$ MPPM for rates above about 0.45 nats/slot (which is the same observation made using the cutoff-rate). Larger values of N and p are needed for MPPM and OPPM to compete with OOK at high rates.

Table 2 summarizes the ultimate limits in throughput (nats/slot) for each modulation scheme. As can be seen, only OPPM can provide throughputs greater than ln(2) nats/slot, but it requires indexes of overlap above $N = 4$ to do so (which will make synchronization significantly more difficult).

3.2 Peak-Power Requirements

Here we investigate the peak power requirements of PPM, MPPM, OPPM and OOK as the data rate r in nats per second increases and uncoded error-probability is kept fixed. We assume a quantum-limited channel. To make the comparison fair between the various modulation schemes, we compare the peak-power needed to convey a sequence of bits through the channel at the same sequence error-probability for each modulation scheme.

MPPM: Remembering that MPPM has p times the average energy per symbol compared to PPM and OPPM (for the same $\lambda_s T_s$) and using the approximate expression for error-probability in (13), we have

$$\lambda_s = \frac{p}{T_s} \ln\left[\frac{p(Q-p)}{(Q-p+1)P(\mathcal{E})}\right] \quad \text{photons/sec.} \tag{50}$$

Substituting $T_s = \ln(M)/Qr$, we obtain

$$\frac{\lambda_s}{r} = \frac{pQ}{\ln(M)} \ln\left[\frac{p(Q-p)}{(Q-p+1)P(\mathcal{E})}\right] \quad \text{photons/nat.} \tag{51}$$

The above expression holds as a special case for PPM by setting $p = 1$.

Clearly, for fixed Q, p and $P(\mathcal{E})$, peak-power increases linearly with the data rate, and thus, to reduce the peak-power requirements, we must minimize the slope (which has units of photons/nat) on the right-hand side of (51).

Another quantity of interest for practical systems is the peak-to-average power, α, which for MPPM is given by $\alpha = Q/p$ (note that $1/\alpha$ is the probability of a pulsed slot in a sequence of data).

OPPM: An expression parallel to (51) relating the peak power requirements of OPPM to the throughput for a fixed error-probability can be similarly derived and is given by

$$\frac{\lambda_s}{r} = \frac{NQ}{\ln[N(Q-1)+1]} \ln\left[\frac{N(Q-1)}{[N(Q-1)+1]P(\mathcal{E})}\right] \quad \text{photons/nat.} \tag{52}$$

The peak-to-average power requirements for OPPM are the same as those for PPM: $\alpha = Q$.

OOK: For OOK (which has an average energy per symbol equal to $\lambda_s T_s/2$), the probability of sequence error for a sequence of L bits is $P(\mathcal{E}) = 1 - [1 - \exp[-2\lambda_s T_s)]^L$. Then,

$$\frac{\lambda_s}{r} = -\frac{\ln\left[1 - [1 - P(\mathcal{E})]^{\frac{1}{L}}\right]}{2\ln(2)} \quad \text{photons/nat.} \tag{53}$$

The peak-to-average power for OOK is $\alpha = 2$.

Table 3 compares the quantity λ_s/r in photons/nat for the various modulation schemes at 2, 3, 4, 5, and 6 bits/symbol and an error-probability of 10^{-3}. For OPPM and MPPM, the parameter values were chosen to yield the best results for the number of bits/symbol required. $N = 2$ for OPPM and $p = 2$ for MPPM were seen to yield the smallest peak powers for a fixed data rate.

The table shows that OOK is by far the best. MPPM is inferior to both PPM and OPPM at two and three bits/symbol but becomes significantly better at the higher rates. PPM is uniformly better than OPPM, although the difference becomes smaller at the higher rates. The latter observation may seem surprising at first glance, since whereas throughput in nats/second for PPM can only increase at the expense of a smaller T_s (which means a larger peak-power λ_s to maintain the same performance), this is not the case for OPPM. On the other hand, OPPM requires larger peak-powers to achieve the same error-probability as PPM, which apparently is the reason for its being inferior compared to the latter.

3.3 Capacity and Cutoff-Rate Comparisons

Here we compare the capacities and cutoff-rates of the various modulation schemes in nats/slot as a function of the average energy per nat.

Figure 7 compares the cutoff-rates in nats/slot for OOK, PPM, OPPM and MPPM. For OPPM we consider $N = 2$ and $N = 3$ which are small enough not to make synchronization impractical, and for MPPM, we consider $p = 2$, $p = 3$, and $p = 4$. The values of Q for PPM, OPPM and MPPM were chosen to maximize the capacity/cutoff-rate at large signal levels, namely $Q = 3$ for PPM, $Q = 2$ for OPPM and $Q = 2p + 1$ for MPPM. The superiority of OOK in this comparison is obvious from the figure. OPPM is inferior to MPPM for small signal levels but becomes better at the higher levels. For $N \geq 4$, OPPM will perform better than OOK as the average number of signal photons increases, since (see Table 2) OOK saturates at $\ln(2)$ nats/slot, whereas OPPM to $\frac{1}{2}\ln(N + 1)$ nats/slot.

A comparison using capacity instead cutoff-rate yields results qualitatively similar to those in Figure 7, which are not presented to save space.

4 Coding

In this section we compare the coded performances of OPPM and MPPM. In the interest of space, this comparison is not exhaustive and is only meant to illustrate what the possibilities are with each modulation scheme. We focus on trellis-coded modulation (TCM), rather than block-coding (and specifically Reed-Solomon coding), which has been previously studied for PPM [1, 20, 21] and MPPM [11]. Some work on TCM for optical OPPM with $Q = 2$ was presented in [8, 22]. Here we present new results for $Q = 4$ OPPM and for MPPM.

4.1 OPPM

We consider two examples of how trellis-coded modulation can be used in conjunction with OPPM to obtain a coding gain and/or increase the throughput. For brevity, we present results only for the quantum-limited channel, but qualitatively similar results were obtained for the background noise channel as well.

The first example, which was also studied in [8], starts with $Q = 2$ PPM, which yields a throughput of 1/2 bits/slot, and has a peak-to-average power ratio of $\alpha = 2$. With an index of overlap $N = 7$, the number of OPPM signals is $J = 8$, which results in a threefold increase in the number of bits per slot from 1/2 to 3/2, while α remains the same. Using a rate 2/3 Ungerboeck code [23] we can trade off some throughput for performance. Figure 8 shows results for the 8 and 16 state Ungerboeck codes with the trellises populated by OPPM instead of phase-shift-keying (PSK) signals [23]. Our reference for comparison is QPPM which has a throughput efficiency of 1/2 bits/slot. We note that the 16-state code is only slightly more than 1dB worse than QPPM at a symbol-error-probability of 10^{-5}. However, the coded OPPM system operates at twice the throughput of QPPM. On the negative side, the coded OPPM system has half the peak-to-average power of QPPM and requires a relatively large index of overlap $N = 7$, which implies more stringent synchronization requirements.

As a second example, we consider OPPM with $Q = 4$. With an index of overlap $N = 3$, we obtain $J = 10$ signals, two of which can be discarded to yield 8 modulation signals. However, a more efficient scheme is to use a fractional index of overlap $N = 7/3$ which also yields eight modulation signals. The throughput efficiency of this scheme is 3/4 bits/slot and a rate 2/3 Ungerboeck code can be used to reduce the rate to 1/2 bits/slot (same as for QPPM) in exchange for a coding gain. Figure 8 shows the performance of the 8 and 16-state Ungerboeck codes using this signal set. It can be seen that the 8-state and 16-state codes are about 2.5 dB and 3.0 dB better than QPPM respectively at an error-probability of 10^{-5}, for the same throughput and peak-to-average power as the latter.

Clearly, even more powerful codes can be designed using this approach that not only give a coding gain but possibly a throughput gain as well at the expense of more complexity. We do not pursue this here as our interest is mainly on getting a flavor of what may be possible.

4.2 MPPM

Here we are interested in coding for MPPM signals at throughputs in bits/slot close to those of QPPM. Also, of interest is the peak-to-average power parameter α which for MPPM is $\alpha = Q/p$.

As indicated above, the minimum Hamming distance for uncoded MPPM signals is two, which is also that for uncoded QPPM. However, whereas QPPM conveys only 2 bits/symbol, MPPM can convey more. Let's compare the performance of uncoded QPPM with that of uncoded MPPM for the same *energy per bit*, μ photons/bit. For QPPM, we have ($\asymp$ means "asymptotically")

$$P(\mathcal{E}) \asymp \exp(-2\mu), \tag{54}$$

and for MPPM (using the approximate expression in (13))

$$P(\mathcal{E}) \asymp \exp(-\frac{\log(M)}{p}\mu). \tag{55}$$

Thus, the gain of MPPM over QPPM is

$$G = 10\log_{10}\left[\frac{\log\binom{Q}{p}}{2p}\right] \leq 10\log_{10}\left[\frac{h(p/Q)}{2(p/Q)}\right], \tag{56}$$

where the bound is in view of (4). It is easy to see that G increases monotonically as p/Q decreases. However, as p/Q decreases, so does the rate in bits/slot: $rT_s = \log[\binom{Q}{p}]/Q \leq h(p/Q)$. If we constrain the rate in bits/slot to be at least $1/2$ (that of QPPM) and the peak-to-average power to be at least 4 (that of QPPM), then $1/4 \geq p/Q \geq h^{-1}(1/2)$. Evidently, the largest gain is obtained for $p/Q = h^{-1}(1/2)$ and is

$$G \leq -10\log_{10}[4h^{-1}(1/2)] \approx 3.56 \text{ dB}, \tag{57}$$

indicating that MPPM can provide some gain even without coding. The 3.56dB gain is the maximum that can be obtained without the use of further coding, and can only be achieved at very large (theoretically infinite) values of Q. As an example of what can practically be achieved, consider $Q = 16$, $p = 4$ MPPM resulting in 1820 signals; this is the example studied in [11]. Deleting enough signals to obtain 1024 signals (10 bits/symbol) it is easy to see that the minimum distance of the 1024 signal constellation is still two, the same as the original constellation; thus (55) still holds by replacing M by 1024. The resulting coding gain over QPPM is 0.969dB, which is what was reported in [11] using simulations. Next we investigate the use of coding over MPPM signals.

It is clearly possible to use only a subset of the MPPM signals for a given Q and p for which the minimum distance is greater than two, at the expense of a throughput reduction. In particular, we are interested in a 3dB gain over QPPM, by insisting that the minimum

Hamming distance for the subset of MPPM symbols be at least four. Table 4 shows the results of a computer search for such codes for different values of Q and p. The table gives the number of MPPM symbols whose distance is at least four, and the rate in bits/slot of a practical code obtained by deleting additional symbols (codewords) in order to obtain a number who is a power of two. This deletion of symbols can be made intelligently in order to facilitate for example synchronization and to relax the strain on the laser (as was discussed for example in [11]). In the interest of space, we do not list the codewords for the codes listed in the table.

As can be seen from the table, it is possible to obtain codes with a 3dB gain over QPPM at rates of 1/2 bits/slot or better and for $\alpha = 4$. The problem is that these are nonlinear codes and efficient techniques for decoding must be found before they can become practical. If the laser can support smaller values of α, then smaller codes can be designed with a 3dB gain over QPPM and the same rate. For example, for $\alpha = 3.2$, a code with a 3dB gain over 256 MPPM symbols and rate 1/2 can be designed. Finally, for $\alpha = 2$, a rate 9/16 code can be designed with $Q = 16$ that has a 3dB gain over QPPM.

For more powerful codes that can be also practically implemented, a concatenated coding scheme where a block or trellis code is used over a set of MPPM symbols (which can be thought of as the inner code) may be necessary. Such an approach was employed in [11] where a Reed-Solomon code was used in conjunction with 1024 MPPM symbols. Here, instead, we investigate briefly the use of trellis-coding over MPPM symbols.

For the example here we use the 8-state Ungerboeck trellis shown in Figure 9 [24]. With $Q = 9$, $p = 2$ MPPM, we have $M = 36$ signals, four of which can be deleted to yield a set of 32 modulation signals. Two of those deleted signals could be those having pulses at the first two and last two slots, to avoid the possibility of the laser being on over four consecutive slots. The other two signals to be deleted can be chosen based on other criteria, such as to help synchronization. The rate of the trellis code is 4/5, which when multiplied by 5/9, the rate in bits/slot of the MPPM signal set, gives an overall rate of 4/9 bits/slot. The peak-to-average power ratio is $\alpha = 4.5$.

The next step is to partition the 32 MPPM symbols into eight subsets of four signals each whose Hamming distance (since as noted above it is the Hamming distance that determines performance) is greater than the minimum of the 32-MPPM constellation. Since for $p = 2$ the two possible signal distances are two and four, this means that the distance between signals in the same subset (which correspond to parallel transitions) must be four. This further implies that the *maximum* free distance of the code is four. Since signals leaving and entering a state have a Hamming distance of at least two, this implies that the *minimum* free distance of the code is four, which combined with the above observation means that the code has a free distance of four. Thus, for the same energy per bit, the code has a 3dB asymptotic coding gain over QPPM. This gain was verified through simulations, as shown in Figure 8.

Figure 9 shows the partitioning of the 32-MPPM signals into subsets $D0$, $D1$, $\cdots$, $D7$. In describing the subsets, an MPPM signal is represented by p numbers ($p = 2$ here) enclosed in parentheses that indicate the bit positions where the pulses are located.

More work on the topic needs to be done to obtain high rate codes (greater than 1/2) that provide good coding gains while satisfying the duty-cycle and peak and average power constraints imposed by the laser.

5 Conclusion

We have studied various aspects of modulation and coding for high rate optical links, by analyzing and comparing the performance of various modulation schemes under different criteria. No modulation scheme considered was seen to be uniformly superior to all other under all constraints and all parameter values. OPPM seems to perform better than MPPM in terms of throughput at small values of Q ($Q = 2$ is best) whereas MPPM's power is evident at the larger values of Q, that result in large signal constellations. On the other hand, with small Q values OPPM requires large indices of overlap for large throughput, which will make synchronization more difficult in a practical implementation. OOK performed very well in most comparisons, especially at the higher rates. Its drawback is that it's not an equal energy signaling scheme (which means that an estimate of the received power is needed by the receiver before decisions are made), and it does not guarantee that long streams of zeros or ones will not occur. PPM was seen to be largely inferior to the other modulation schemes.

All modulation schemes studied in this paper were obtained by imposing block constraints on binary sequences, i.e., sequences of these modulation symbols are subsets of the set of all possible OOK sequences. It is thus entirely possible (if not certain) that one can start with OOK and by more judiciously imposing constraints produce schemes that operate at higher rates than the modulation schemes studied here.

References

[1] J.R. Lesh, J. Katz, H.H. Tan, and D. Zwillinger, "2.5 Bits/Detected Photon Demonstration Program: Description, Analysis, and Phase I Results," TDA Report 42-66, pp. 115-132, Jet Propulsion Laboratory, Pasadena, CA, December 1981.

[2] J.R. Pierce, "Optical Channels: Practical Limits with Photon Counting," IEEE Transactions on Communications, Vol. COM-26, pp. 1819-1821, December 1978.

[3] D.L. Snyder and I.B. Rhodes, "Some Implications of the Cutoff Rate Criterion for Coded Direct-Detection Optical Communications Systems," IEEE Transactions on Information Theory, vol. IT-26, pp. 327-338, July 1981.

[4] X. Sun and F. Davidson, "Direct-Detection Optical Intersatellite Link at 220 Mbps Using AlGaAs Laser Diode and Silicon APD with 4-ary PPM Signaling," NASA CR-186380, 1990.

[5] J.M. Budinger, S.D. Kerslake, L.A. Nagy, M.J. Shalkhauser, N.J. Soni, M.A. Cauley, J.H. Mohamed, J.B. Stover, R.R. Romanofsky, P.J. Lizanich, and D.J. Mortensen, "Quaternary Pulse-Position Modulation Electronics for Free-Space Laser Communications," NASA Technical Memorandum 104502, NASA Lewis Research Center, September 1991.

[6] G.M. Lee and G.W. Schroeder, "Optical Pulse-Position Modulation with Multiple Positions per Pulsewidth," IEEE Transactions on Communications, Vol. COM-25, pp. 360-364, March 1977.

[7] I. Bar-David and G. Kaplan, "Information Rates of Photon Limited Overlapping Pulse Position Modulation Channels," IEEE Transactions on Information Theory, Vol. IT-30, pp. 455-464, May 1984.

[8] C.N. Georghiades, "Some Implications of TCM for Optical Direct-Detection Channels," IEEE Transactions on Communications, Vol. 37, No.5, pp. 481-487, May 1989.

[9] C.N. Georghiades and J.K. Crutcher, "Throughput Efficiency Considerations for Optical OPPM," *Proceedings of the Global Telecommunications Conference*, Phoenix, AZ, November 1991.

[10] H. Sugiyama and K. Nosu, "MPPM: A Method of Improving the Band-Utilization Efficiency in Optical PPM," Journal of Lightwave Technology, vol. 7, No. 3, March 1989.

[11] James M. Budinger, Mark Vanderaar, P. Wagner. and Steven Bibyk, "Combinatorial Pulse Position Modulation for Power-Efficient Free-Space Laser Communications," SPIE Proceedings, Vol. 1866, January 20-21, 1993.

[12] T.M. Cover and J.A. Thomas, *Elements of Information Theory*, Wiley, New York, 1991.

[13] T. Ohtsuki, H. Yashima, I. Sasase and S. Mori, "Cutoff-Rate and Capacity of MPPM in Noisless Photon Counting Channel," IEICE Transactions, vol. E 74, No. 12, December 1991.

[14] J.R. Lesh, W.K. Marshall and J. Katz, "Simple Method for Designing or Analyzing an Optical Communication Link," Proceedings of the Military Communications Conference, 1986.

[15] Robert G. Gallager, *Information Theory and Reliable Communication,* Wiley, New York, 1968.

[16] J.M. Wozencraft and R.S. Kennedy, "Modulation and Demodulation for Probabilistic Coding," IEEE Transactions on Information Theory, vol. IT-12, pp. 291-297, July 1966.

[17] J.L. Massey, "Coding and Modulation in Digital Communications," in Proceedings of the International Zurich Seminar in Digital Communications, Zurich, Switzerland, March 1974.

[18] S.A. Butman, J. Katz and J.R. Lesh, "Bandwidth Limitations on Noiseless Optical Channel Capacity," IEEE Transactions on Communications, vol. COM-30, pp. 1262-1264, May 1982.

[19] D.L. Snyder and C.N. Georghiades, "Design of Coding and Modulation for Power-Efficient Use of a Band-Limited Optical Channel," IEEE Transactions on Communications, vol. COM-31, pp. 560-565, April 1983.

[20] R.J. McEliece, "Practical Codes for Photon Communication," IEEE Transactions on Information Theory, vol. IT-27, pp. 393-398, July 1981.

[21] J.L. Massey, "Capacity, Cutoff-Rate and Coding for a Direct-Detection Optical Channel," IEEE Transactions on Communications, vol. COM-29, pp. 1615-1621, November 1981.

[22] G.J. Pottie, "Trellis Codes for the Optical Direct-Detection Channel," IEEE Transactions on Communications, vol. 39, pp. 1182-1183, August 1991.

[23] G. Ungerboeck, "Channel Coding with Multilevel/phase Signals," IEEE Transactions on Information Theory, vol. IT-28, pp. 55-67, January 1982.

[24] G. Ungerboeck, "Trellis-Coded Modulation with Redundant Signal Sets Part I: Introduction," IEEE Communications Magazine, Vol. 25, No. 2, February 1987.

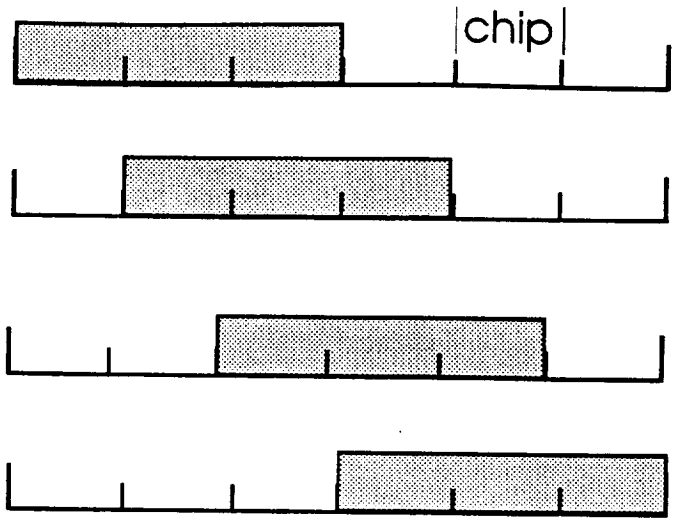

Figure 1: An example of OPPM for $Q = 2$, $N = 3$.

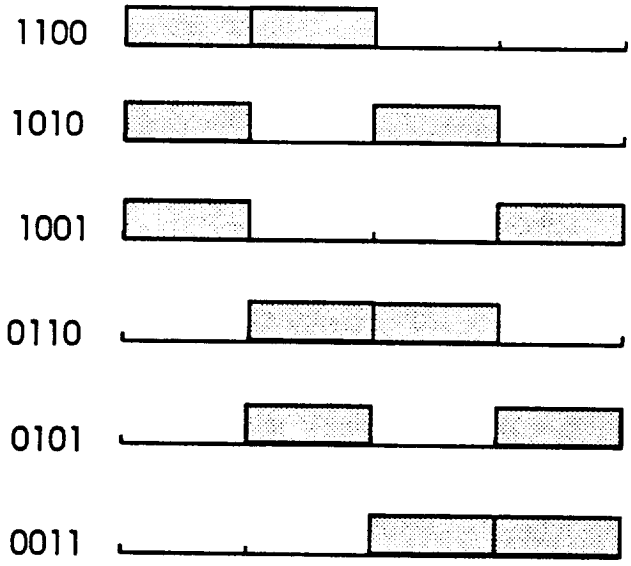

Figure 2: An example of MPPM for $Q = 4$, $p = 2$.

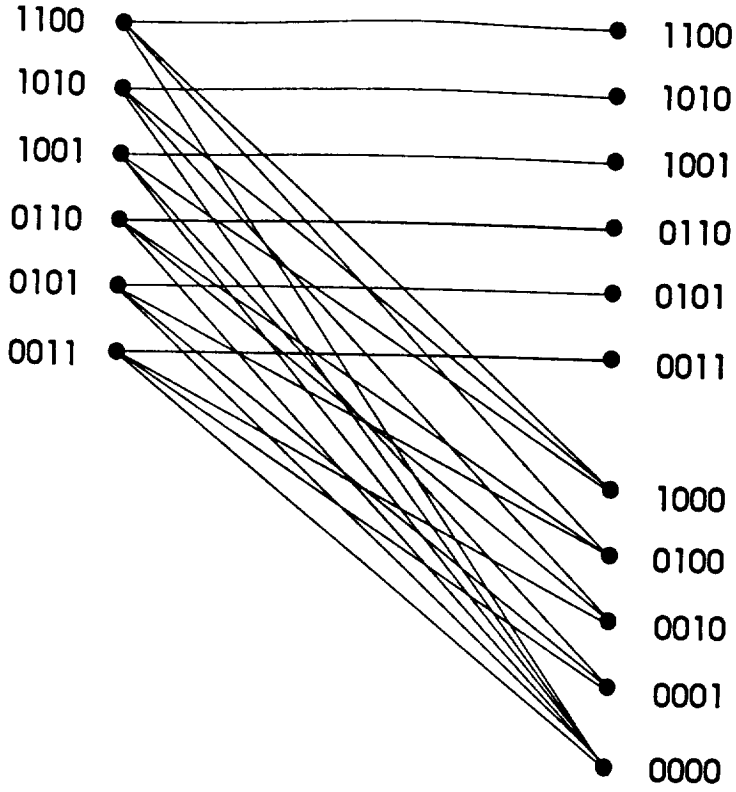

Figure 3: The DMC model for (4,2)-MPPM.

Table 1: Capacity in Nats/Photon. The numbers in parentheses for MPPM and OPPM correspond to the optimum values of Q, and for OOK, to a uniform prior distribution.

rT_s nats/slot	C_{ph}, PPM nats/photon	C_{ph}, $p = 2$ MPPM nats/photon	C_{ph}, $N = 2$ OPPM nats/photon	C_{ph}, OOK nats/photon
0.10	1.859 (16)	2.055 (35)	1.998 (18)	0.697 (0.663)
0.15	1.423 (10)	1.642 (23)	1.589 (12)	0.676 (0.647)
0.20	1.102 (7)	1.343 (16)	1.297 (9)	0.654 (0.629)
0.25	0.833 (5)	1.103 (13)	1.069 (7)	0.631 (0.609)
0.30	0.598 (4)	0.898 (10)	0.877 (6)	0.606 (0.588)
0.35	0.337 (3)	0.711 (8)	0.716 (5)	0.579 (0.564)
0.40	—	0.523 (7)	0.579 (4)	0.550 (0.538)
0.45	—	0.284 (5)	0.437 (3)	0.518 (0.509)
0.50	—	—	0.318 (3)	0.482 (0.476)
0.55	—	—	—	0.441 (0.436)
0.60	—	—	—	0.390 (0.388)
0.65	—	—	—	0.320 (0.319)

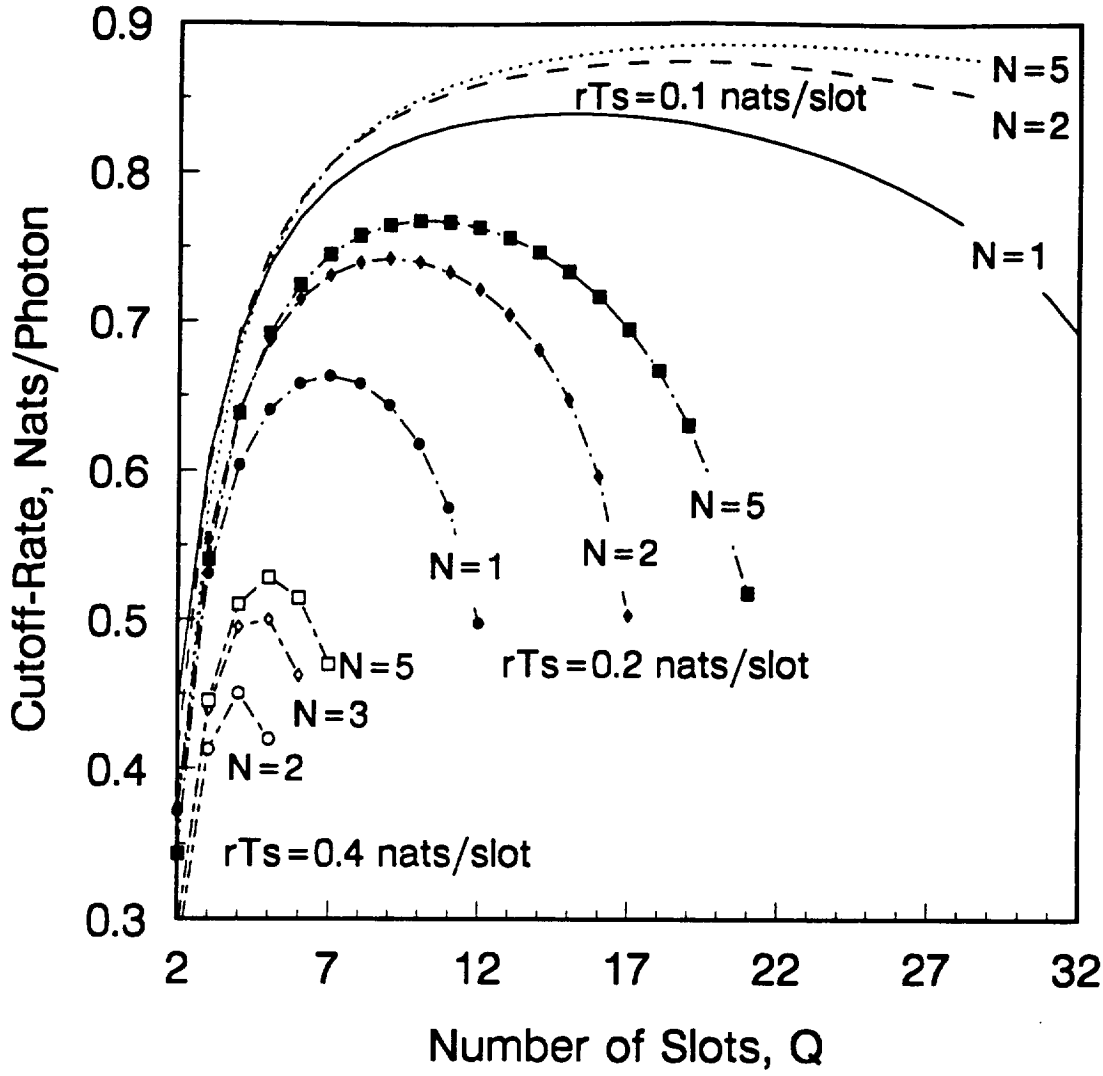

Figure 4: Nats per photon as a function of Q for OPPM various rT_s in nats/slot.

Table 2: Throughput limitations in nats/slot.

OOK	PPM	MPPM	OPPM
$rT_s \leq \ln(2)$	$rT_s \leq \frac{\ln(3)}{3}$	$h(p/Q) - \frac{\ln(1+Q)}{Q} \leq rT_s \leq h(p/Q)$	$rT_s \leq \frac{\ln(N+1)}{2}$
	equality for $Q = 3$	equality for $Q = \infty$	equality for $Q = 2$

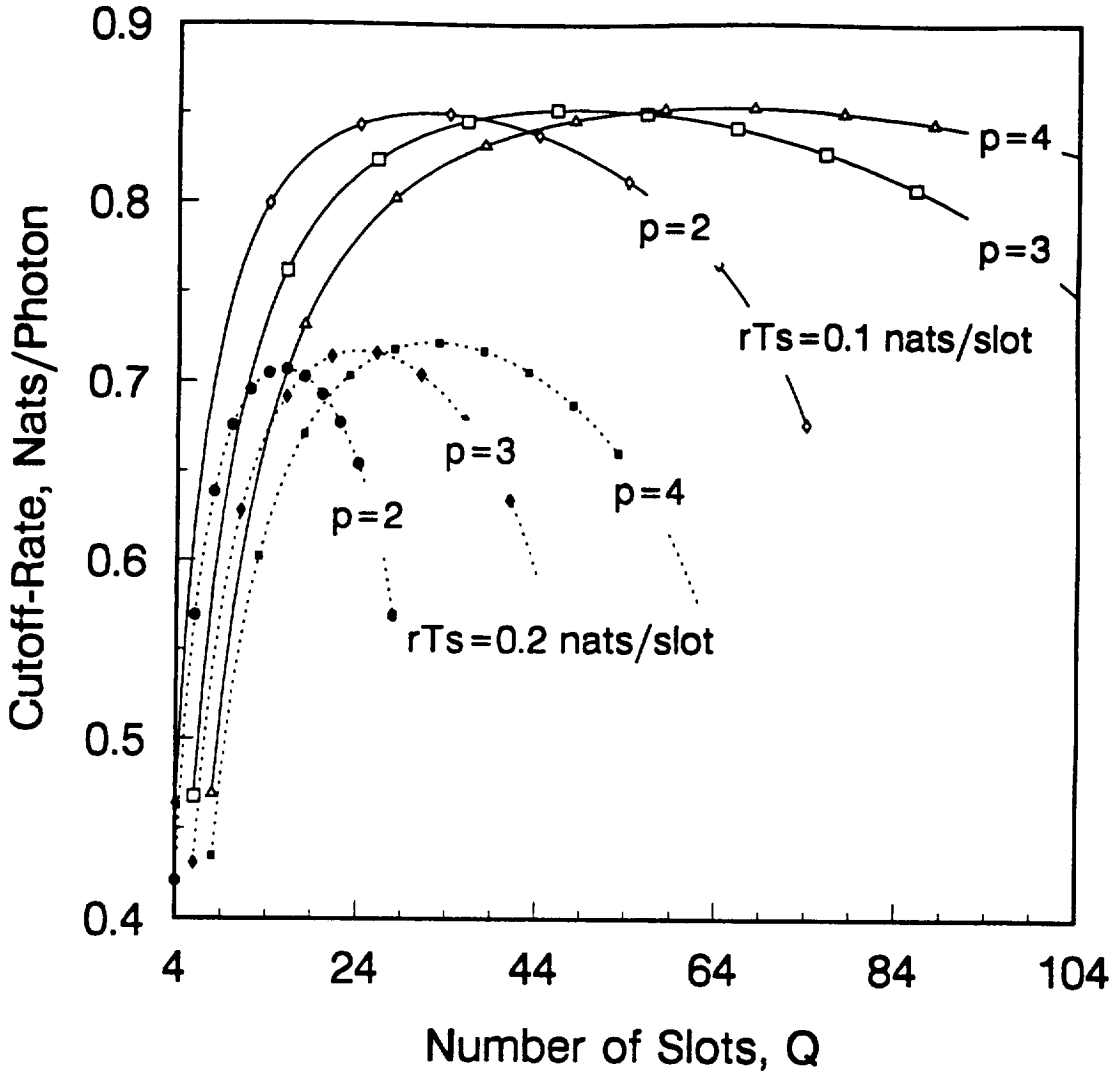

Figure 5: Nats per photon as a function of Q for MPPM various rT_s in nats/slot.

Table 3: Peak-power performance in photons/nat at an error-probability of 10^{-3}.

OOK		PPM		OPPM		MPPM	
2^L	λ_s/r	Q	λ_s/r	Q,N,J	λ_s/r	Q,p,M	λ_s/r
4	5.48	4	19.10	3,2,5	24.92	5,2,10	31.76
8	5.780	8	26.06	5,2,10	30.90	5,2,10	31.76
16	5.98	16	39.49	9,2,17	43.50	7,2,21	34.11
32	6.14	32	63.49	17,2,33	66.87	12,2,66	42.99
64	6.27	64	106.06	33,2,65	108.97	12,2,66	42.99

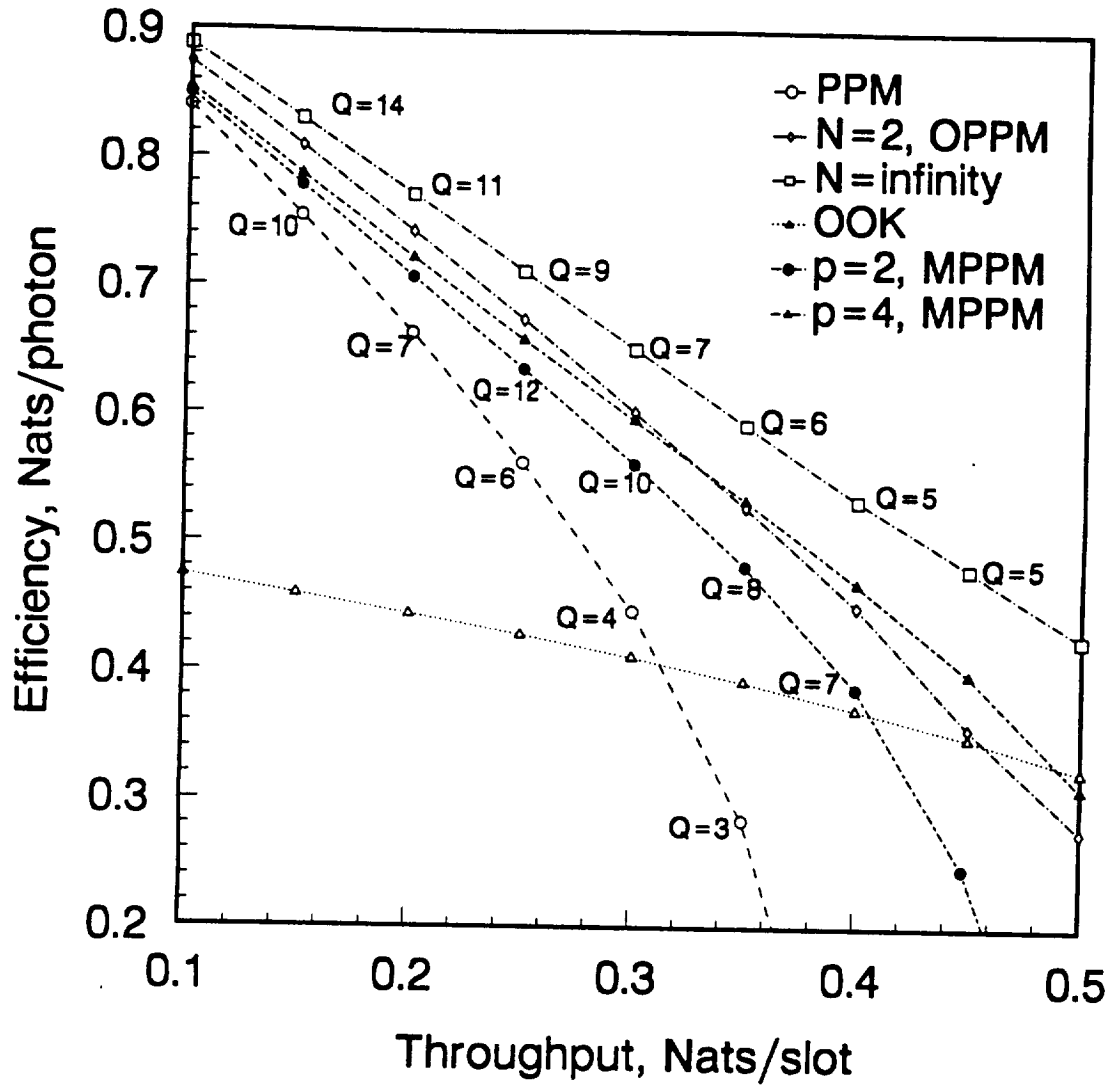

Figure 6: Nats/photon as a function of rT_s for the various modulation schemes. The values of Q shown for PPM, OPPM and MPPM result in the largest efficiencies.

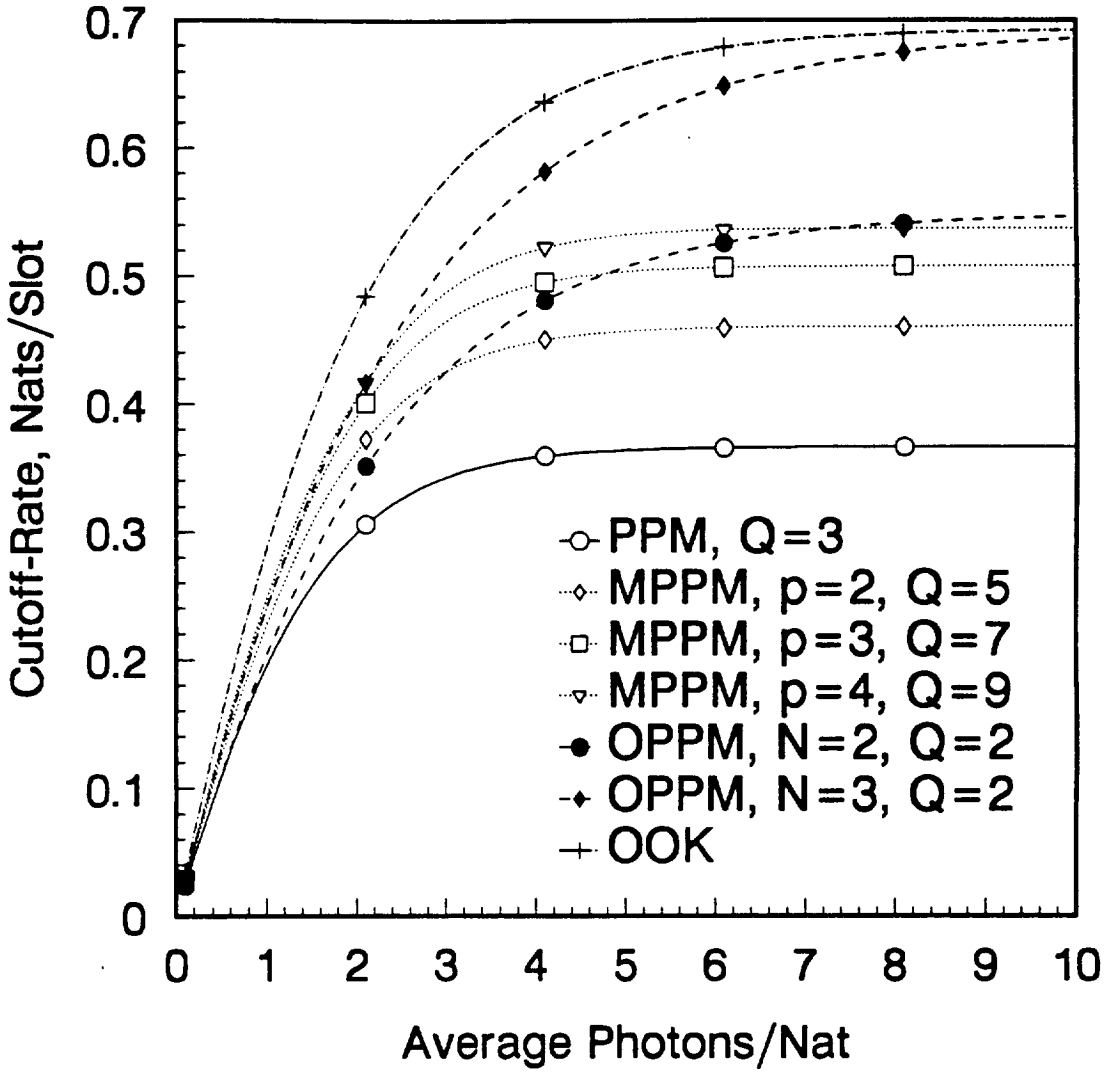

Figure 7: Comparison of cutoff-rates in nats/slot.

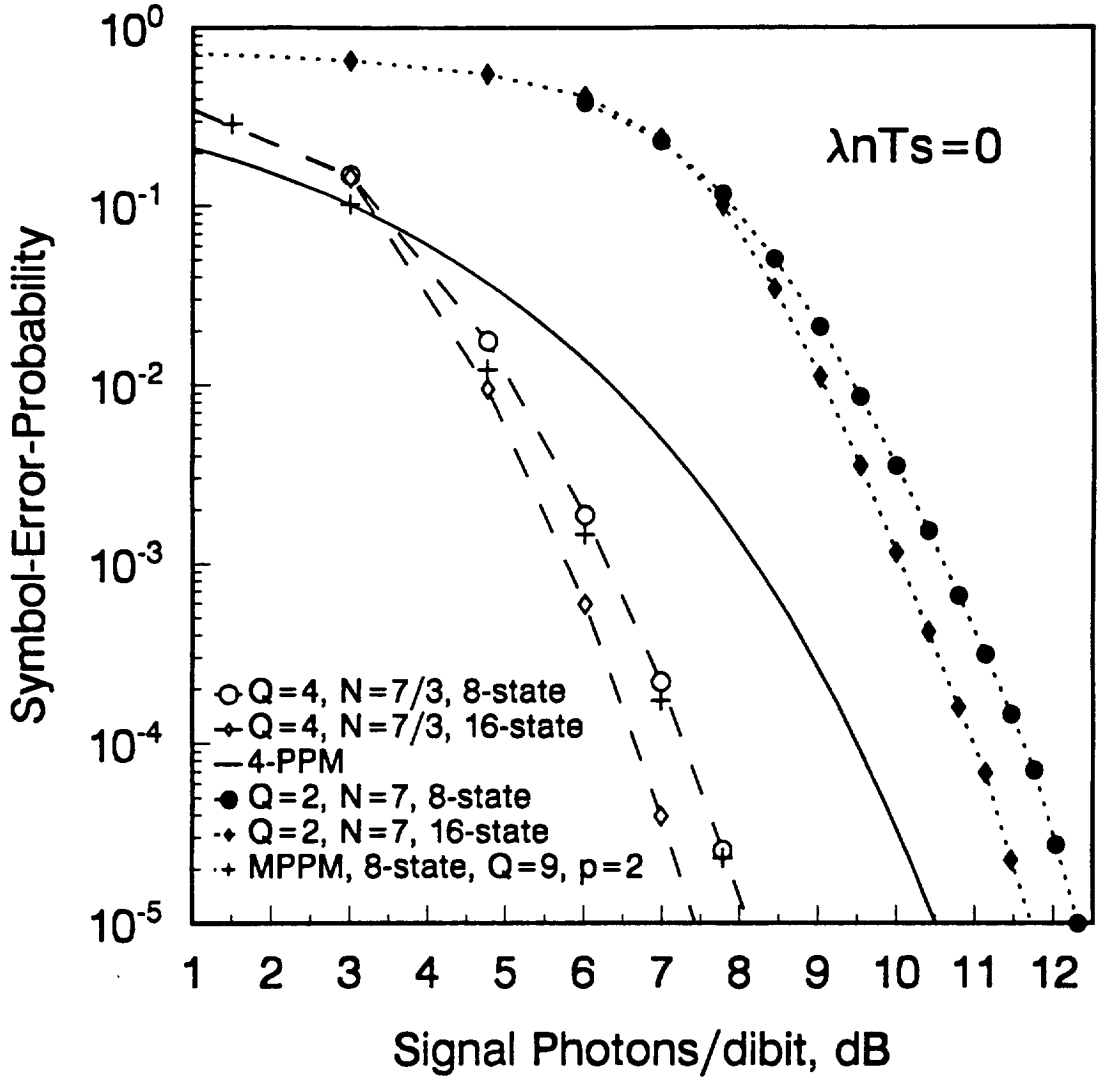

Figure 8: Symbol-error probability for trellis-coded OPPM and MPPM compared to QPPM.

Table 4: Various coding rates for MPPM signal sets with minimum Hamming distance of four.

Q, p, α	Number of Symbols	Code Rate
$Q = 24,\ p = 6,\ \alpha = 4$	4316	1/2
$Q = 28,\ p = 7,\ \alpha = 4$	37202	15/28
$Q = 16,\ p = 5,\ \alpha = 3.2$	273	1/2
$Q = 18,\ p = 6,\ \alpha = 3$	756	1/2
$Q = 12,\ p = 6,\ \alpha = 2$	68	1/2
$Q = 14,\ p = 7,\ \alpha = 2$	232	1/2
$Q = 16,\ p = 8,\ \alpha = 2$	870	9/16

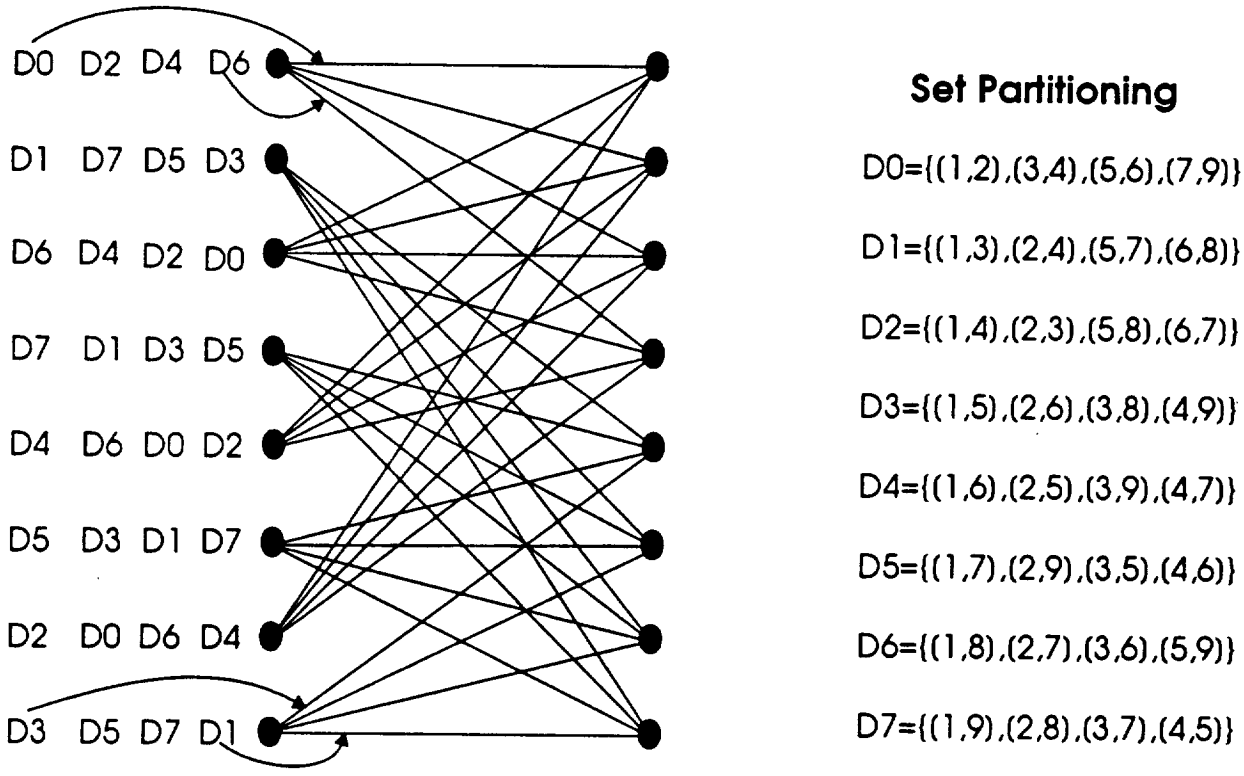

Figure 9: The trellis for the 8-State code used with the 32 MPPM signals and the subsets resulting from set-partitioning: $Q = 9$, $p = 2$.